Modeling of Amplitude Squeezing in a Pump-Noise-Suppressed Interband Cascade Laser

Shiyuan Zhao and Frédéric Grillot, *Senior Member, IEEE*

Abstract—A semi-classical rate equation model for the amplitude squeezing of mid-infrared interband cascade lasers is presented based on Green's function method. We analytically investigate the squeezing performance through a small signal analysis, where an additional partition noise in the output power is considered because of the anti-correlation between photons reflected and transmitted at the output laser facet. Thus, the squeezing effect can be achieved in the low frequency region with noise-suppressed pump. Amplitude squeezed states in interband cascade lasers can qualitatively be evaluated depending on the pump noise conditions. Such ultra-low amplitude noise laser sources enable various applications such as high precision measurements, metrology, and spectroscopy range where squeezed states can be used to replace current shot-noise limited laser mid-infrared sources.

Index Terms—Semiconductor lasers, relative intensity noise, amplitude squeezing light, mid-infrared sources.

I. INTRODUCTION

NON-CLASSICAL or "squeezed" state of light has been widely studied over the last few decades [1]–[3]. The so-called "squeezed" state has less fluctuations in one quadrature component than a coherent state but at the expense of increased fluctuations in the other quadrature components due to the Heisenberg's uncertainty relation. In quantum physics, coherent states usually have equal variance for each of the two quadrature components, while the quadrature variances of the squeezed states are not equal but the minimum-uncertainty relationship is still preserved. Consequently, as observed in this experiment, the noise level of these squeezed fields can be reduced below the shot-noise limit, which is featured by the coherent fields. Squeezed states of light offer intriguing potentials in different types of applications, such as quantum optical communications [4], precision measurements for gravitational wave [5] and quantum sensing [6]. The generation of squeezing light from a semiconductor laser has several significant advantages over other methods. Amplitude-squeezed states of light generated

from semiconductor lasers exhibit a wideband squeezing, intense optical power, and narrow frequency linewidth. Also, semiconductor lasers can generate brightly squeezed light rather than squeezed vacuum light namely because the squeezing is set up on large steady-state optical fields. The initial experimental production of squeezed states directly from semiconductor lasers was demonstrated by Yamamoto *et al.* [7], which showed the possibility of generating intensity squeezing light with high-impedance suppression for pump-amplitude fluctuation. Therefore, squeezed states can be used to replace current shot-noise-limited laser sources in many applications where ultralow laser noise below the standard quantum limit is required. Additionally, for many applications, such as quantum key distribution with entangled photons, a large squeezing bandwidth is also desirable for achieving high-speed communications. Finally, recent studies also reveal the feasibility of squeezing generation method on cavity-enhanced nanolasers [8].

In this work, we address a novel class of quiet-light optoelectronic devices operating in the mid-infrared window in which the photon-number fluctuations are suppressed below normal shot-noise levels. To this end, interband cascade lasers (ICLs) emitting in a broad wavelength range of 3-6 μm are considered. The active region is usually composed of many stage cascade periods of type-II quantum wells (QW). As shown in Fig. 1, ICLs combine the relatively long upper-level recombination lifetime and the power-efficient cascading mechanism which can generate coherent light via interband transitions [9]. Consequently, their active medium is different from that of quantum cascade lasers (QCLs) in which photons are emitted from intersubband transitions. On top of that, the power consumption of ICLs is one or two orders of magnitude lower than the QCL counterparts which is meaningful for applications for a variety of applications, such as gas sensing, free space communication, optical frequency comb and ICLs incorporated into photonics integrated circuits [10]–[12]. As for the theoretical description of squeezing light in semiconductor lasers, it was initially proposed by Yamamoto *et al.* in the case of Fabry-Perot semiconductor lasers by using a fully quantum mechanical based model [13] consistent with experimental results [7].

Although quantum fluctuations of optical fields are perfectly described by the formalism of quantum electrodynamics (QED), such rigorous quantum approach becomes laborious and sometimes especially complicated. Several authors [14]–[17] then introduced alternative semi-classical methods which give correct

Shiyuan Zhao is with the LTCI, Télécom Paris, Institut Polytechnique de Paris, 91120 Palaiseau, France (e-mail: shiyuan.zhao@telecom-paris.fr).

Frédéric Grillot is with the LTCI, Télécom Paris, 91120 Palaiseau, France, and also with the Center for High Technology Materials, The University of New Mexico, Albuquerque, NM 87106 USA (e-mail: grillot@telecom-paristech.fr).
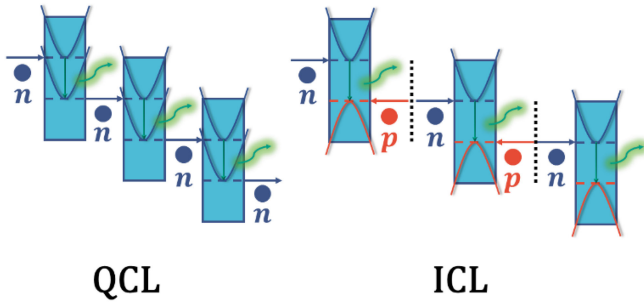
Fig. 1. Schematic diagrams of the carrier injection process. Electron injection is indicated with dark blue arrows, and hole injection with red arrows. Photon emission is indicated with green arrows. Blue (red) dashed lines stand for subbands in the conduction (valence) bands. The diagrams are shown for a QCL on the left and an ICL on the right.

pictures of the noise compression phenomena, while avoiding the computational complications of rigorous QED processing. For example, Marcenac and Caroll [16], based on the transmission line method [14], introduces vacuum fluctuations to describe the process of generation of amplitude-squeezing light. Jacques Arnaud [17] has developed a classical corpuscular theory that does not require quantization of the electromagnetic field which perfectly coincides with the quantum counterparts. In this paper, our formalism is developed with the assumptions that the fundamental source of noise resides in the particle character of the radiation and in the random instants of the arrival of photons, which do not communicate with each other. Shot-noise is therefore an intrinsic property of radiation other than a property of the light-matter interaction. Hence, laser facet losses regarded as the shot noise source are assimilated to the mirror partition noise due to the photon's particle-like behaviors. It is worth mentioning that our model remains semi-classical because photons are considered as classical particles and without mutual interaction. However, it allows a qualitative and simple description of the amplitude-squeezing light of semiconductor lasers.

The applicability of all these mathematical methods is limited to standard semiconductor lasers, thus, few attentions have been paid to amplitude-squeezing in novel light sources like ICLs [18]. In this article, we deploy Green's function method for generalizing the rate equations of ICLs. Based on such works, we expand a recently developed rate equation approach [19] to the case of squeezing generation, where the accurate studies of squeezed light can be analytically performed. It is worth mentioning that, in comparison with the prior works, we take into consideration the negatively correlated partition noise caused by the laser's out-coupling process, which is of paramount importance and is often referred to as standard quantum limit or shot-noise limit. Importantly, we predict that ICLs are preferable devices for this purpose because large amplitude noise reduction is attainable through inherent high quantum efficiency.

II. GREEN'S FUNCTION METHOD

The Green's function method was initially proposed by Henry [20] and has been studied in the past few years in the context of

semiconductor lasers with complex cavity [21]–[22]. The rigorous study of a semiconductor laser requires a three-dimensional study of the field and its propagation. In this work, we make a number of assumptions. Firstly, the cavity medium is assumed to be isotropic and the matrix propagation equation is reduced to the Helmholtz scalar equation. Secondly, we assume that in the laser, optical waves propagate primarily along the z longitudinal axis and the transverse and lateral axes are neglected. Lastly, the spontaneous emission is delta-correlated in space and time.

A. Generalized Rate Equation

The complex Fourier component $E_\omega(z)$ is governed by the one-dimensional scalar wave equation:

$$\nabla_z^2 E_\omega(z) + k_0^2 \varepsilon E_\omega(z) = F_\omega(z) \tag{1}$$

where $\nabla_z^2 = \frac{\partial^2}{\partial z^2}$ is the Laplacian operator for the longitudinal coordinate z, ω is the lasing angular frequency, $k_0 = \frac{\omega}{c}$ is the wavenumber, c is the velocity of light in vacuum, ε is the complex dielectric constant and $F_\omega(z)$ is the Langevin noise term accounting for the distributed spontaneous emission. Equation (1) may be solved by using the Green's function method [20]:

$$(\nabla_z^2 + k_0^2 \varepsilon) G_\omega(z, z') = \delta(z - z') \tag{2}$$

where $\delta(z - z')$ is the Dirac delta function. Then, the general solution is obtained through a spatial integration of the Green's function weighted by the correspondent excitation source over the total cavity length L:

$$E_\omega(z) = \int_{(L)} dz' G_\omega(z, z') F_\omega(z') \tag{3}$$

The Green's function $G_\omega(z, z')$ has been discussed at length [23] and its one-dimensional formula is given by:

$$G_\omega(z, z')$$
$$= \frac{Z_R(z)Z_L(z')\Theta(z - z') + Z_R(z')Z_L(z)\Theta(z' - z)}{W(\omega, N)} \tag{4}$$

Here $\Theta(z)$ is the Heaviside step function. $Z_L(z)$ and $Z_R(z)$ are two independent solutions of the homogeneous wave equation (i.e., with $F_\omega = 0$), which satisfy the boundary condition at the left laser facet or the right laser facet, respectively.

$W(\omega, N)$ is the explicitly z-independent Wronskian operator of these two solutions defined as [23]:

$$W(\omega, N) = Z_L(z)\frac{d}{dz}Z_R(z) - Z_R(z)\frac{d}{dz}Z_L(z) \tag{5}$$

We know that the laser's longitudinal mode corresponds to a zero point of the Wronskian operator $W(\omega_0, N_{th}) = 0$. Both the lasing frequency ω_0 and the carrier density N_{th} at threshold are determined from this relation. Because the semiconductor laser is assumed to operate only in one longitudinal mode with a field distribution denoted by $Z_L(z) = Z_R(z) = Z_0(z)$, (3) can be rewritten as:

$$\frac{E_\omega(z)}{Z_0(z)} = \frac{1}{W(\omega, N)} \int_{(L)} Z_0(z') F_\omega(z') dz' \tag{6}$$

As the Wronskian operator W is a function of two independent variables ω and N, its expansion about the operating point can be written as:

$$W = \frac{\partial W}{\partial \omega}\Big|_{\omega_0, N_{th}}(\omega - \omega_0)$$
$$+ \frac{1}{L}\int_{(L)}\frac{\partial W}{\partial N}\Big|_{\omega_0, N_{th}}(N - N_{th})dz \quad (7)$$

By using (6)–(7) and the inverse Fourier transform, the rate equation for the electrical field $\beta_0(t)$ is then obtained as:

$$\frac{d\beta_0(t)}{dt} = -\frac{j}{L}\int_{(L)} W_N(N - N_{th})dz \times \beta_0(t) + F(t) \quad (8)$$

where $W_N = (\frac{\partial W}{\partial N})/(\frac{\partial W}{\partial \omega})$ and $F(t)$ is the Langevin force associated with the complex amplitude in the time domain. In addition, $\beta_0(t)$ represents the slowly varying envelope of the electrical field in the laser cavity:

$$\beta_0(t) = \frac{1}{2\pi}\int_{-\infty}^{+\infty}\beta_\omega e^{j\omega t}d\omega \quad (9)$$

where $\beta_\omega = E_\omega(z)/Z_0(z)$. The resolution leads to two generalized differential equations for the photon density P and the phase Φ defined via $\beta_0(t) = \sqrt{P(t)}e^{j\Phi(t)}$:

$$\frac{dP}{dt} = \frac{2}{L}\int_{(L)} Im(W_N)(N - N_{th})dz \times P(t) + F_{P'}(t)$$

$$\frac{d\Phi}{dt} = -\frac{1}{L}\int_{(L)} Re(W_N)(N - N_{th})dz + F_{\Phi'}(t) \quad (10)$$

where Re stands for the real part of the complex force and Im for the imaginary part. Through these generalized equations, both static and dynamic behaviors of any type of semiconductor lasers (both interband and intersubband) can be analyzed, including those made with complex structures such as multisection devices.

Moreover, the well-known Petermann excess noise K factor can be generally defined as [29]:

$$K = \frac{\left(\int_0^L |Z_0(z)|^2 dz\right)^2}{\left|\int_0^L Z_0^2(z)dz\right|^2} \quad (11)$$

From a general viewpoint, the K-factor allows to calculate the enhanced spontaneous emission rate in the lasing mode of semiconductor lasers. Most importantly, as discussed later on, it also takes into account the spatial longitudinal inhomogeneities of the cavity, which can influence the amplitude-squeezing performance.

B. Application to Interband Cascade Lasers

In this article, we focus on a Fabry-Perot ICLs cavity design with power facet reflectivity R_1 and R_2. The field intensity distribution is assumed almost uniform inside the cavity, hence
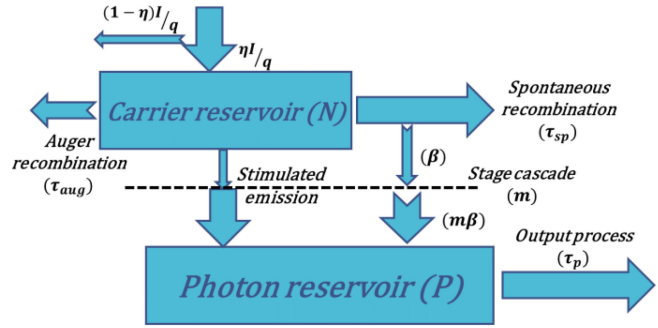

Fig. 2. Reservoir model used in the rate equation analysis of the ICL. Each arrow in the flowchart represents the number of particles flowing per unit of time.

the spatial hole burning effects are neglected. Consequently, the Wronskian operator is then written as [21], [24]:

$$W(\omega, N) = -2jke^{jkL}[1 - r_1 r_2 e^{-2jkL}] \quad (12)$$

Then the partial derivative of the Wronskian is [24]:

$$W_N = \frac{1}{2}(1 + j\alpha_H)\Gamma_p v_g \frac{\partial g}{\partial N} \quad (13)$$

where $\frac{\partial g}{\partial N} = \frac{a_0}{A}$ is the differential gain [19], a_0 the gain coefficient, A the area of the active region, α_H the linewidth enhancement factor, v_g the group velocity and Γ_p the confinement factor taking into account the fraction of the optical power in the active region. Therefore, the complete description of the ICL structure becomes entirely described by the Wronskian operator.

In this case, the photon and phase rate equations per gain stage can be transformed as:

$$\frac{dP}{dt} = \Gamma_p v_g \frac{\partial g}{\partial N}(N - N_{th})P + F_{P'}(t)$$

$$\frac{d\Phi}{dt} = \frac{1}{2}\alpha_H\Gamma_p v_g \frac{\partial g}{\partial N}(N - N_{th}) + F_{\Phi'}(t)$$

According to the ICL's laser structure in Fig. 2, taking into account the spontaneous emission and the relation between carrier number at transparency N_0 and carrier number at threshold N_{th}, the rate equations for the total photon number P and phase Φ of all gain stages are given by:

$$\frac{dP}{dt} = m\Gamma_p v_g \frac{\partial g}{\partial N}(N - N_0)P - \frac{P}{\tau_p} + m\beta\frac{N}{\tau_{sp}} + F_P(t) \quad (14)$$

$$\frac{d\Phi}{dt} = \frac{1}{2}\alpha_H\left[m\Gamma_p v_g \frac{\partial g}{\partial N}(N - N_0) - \frac{1}{\tau_p}\right] + F_\Phi(t) \quad (15)$$

where m is the number of cascading gain stage, τ_p the photon lifetime and β the spontaneous emission factor. This formalism is equivalent to the recently developed rate equation approach [19].

Additionally, it is well-known that the dynamic evolution of the carrier number per gain stage is governed by the usual relation [22]:

$$\frac{dN}{dt} = \eta\frac{I}{q} - \frac{N}{\tau_e} - GP(t) \quad (16)$$

where $N(t)$, τ_e, η and I are the carrier number within the active zone, the carrier lifetime, the injection efficiency and the pump current, respectively. The optical gain G of the ICL in the active region is linked to the carrier density through the relation:

$$G(N) = \Gamma_p v_g \frac{\partial g}{\partial N}(N - N_0) \qquad (17)$$

For the ICL, the carrier lifetime τ_e is mainly determined by the Auger recombination τ_{aug} and the spontaneous emission τ_{sp} [25]. Thus,

$$\frac{1}{\tau_e} = \frac{1}{\tau_{aug}} + \frac{1}{\tau_{sp}}$$

In case of a Fabry-Perot structure, the Petermann excess noise K factor is derived such as [20]:

$$K = \left(\frac{(R_1 + R_2)(1 - R_1 R_2)}{2 R_1 R_2 \ln(R_1 R_2)} \right)^2 \qquad (18)$$

III. Theory of Relative Intensity Noise

A. Intra-Cavity Relative Intensity Noise

This section investigates the relative intensity noise (RIN) performance through the Langevin approach, which is conducted by the inclusion of the Langevin noise forces [26]. Given that, we introduce $F_N(t)$ and $F_P(t)$ as Langevin noise terms into the carrier and photon rate (14) and (16), respectively. These noise sources are assumed to be white noise (see Appendix 13 in [26]):

$$\frac{d}{dt}(dN) = -\rho_{11} dN - \rho_{12} dP + F_N(t) \qquad (19)$$

$$\frac{d}{dt}(dP) = \rho_{21} dN - \rho_{22} dP + F_P(t) \qquad (20)$$

where

$$\rho_{11} = \frac{1}{\tau_{sp}} + \frac{1}{\tau_{aug}} + \Gamma_p v_g \frac{\partial g}{\partial N} P, \quad \rho_{12} = \Gamma_p v_g \frac{\partial g}{\partial N}(N - N_0)$$

$$\rho_{21} = m \Gamma_p v_g \frac{\partial g}{\partial N} P + m \frac{\beta}{\tau_{sp}}, \quad \rho_{22} = \frac{1}{\tau_p}$$

$$- m \Gamma_p v_g \frac{\partial g}{\partial N}(N - N_0)$$

Furthermore, the correlation strength of noise sources is $\langle F_i(t) F_j(t') \rangle = D_{ij} \delta(t - t')$, where indexes i, j refer to N and P where D_{ij} is the diffusion coefficient between two noise sources that are delta-correlated. Fig. 2 briefly explains the traditional reservoir model in order to characterize the laser noise performance. Pumped electrons are injected into the laser structure (I/q), of which only a certain fraction ($\eta I/q$) arrive in the active region. Then, once in the carrier reservoir, some of them recombine non-radiatively (Auger) while others do it spontaneously. It is worth mentioning that a certain fraction of photons from spontaneous emission does contribute to the lasing mode. These photons, together with those issued from stimulated emission, are further amplified thanks to the cascade stages m provided by the ICL structure. The photon reservoir provides a complete description of such stimulated and spontaneous emission process. Photons leaving the cavity after one round

trip are then controlled through the cavity photon lifetime τ_p leading to a steady output power.

Following the analysis of particle flows into/out of the different reservoirs in [26], the diffusion coefficients can be derived as:

$$D_{NN} = \eta \frac{I}{q} + \frac{N}{\tau_{aug}} + \frac{N}{\tau_{sp}} + \Gamma_p v_g \frac{\partial g}{\partial N}(N - N_0)P$$

$$D_{PP} = m \Gamma_p v_g \frac{\partial g}{\partial N}(N - N_0)P + \frac{P}{\tau_p} + m\beta \frac{N}{\tau_{sp}}$$

$$D_{NP} = D_{PN} = -\left[m\beta \frac{N}{\tau_{sp}} + m\Gamma_p v_g \frac{\partial g}{\partial N}(N - N_0)P \right]$$

Applying a small-signal analysis to the rate (19) and (20), one can obtain the linearized equations through Fourier transform:

$$\begin{bmatrix} \rho_{11} + j\omega & \rho_{12} \\ -\rho_{21} & \rho_{22} + j\omega \end{bmatrix} \begin{bmatrix} \delta N(\omega) \\ \delta P(\omega) \end{bmatrix} = \begin{bmatrix} F_N(\omega) \\ F_P(\omega) \end{bmatrix} \qquad (21)$$

Then, as a consequence of this matrix, it becomes straightforward that the intra-cavity relative intensity noise (RIN) corresponds to the definition by using Cramer's rule:

$$RIN_{in}(\omega) = \frac{\langle \delta P(\omega) \delta P(\omega)^* \rangle}{P^2} = \frac{1}{P^2 |\Omega|^2} (\alpha + \beta \omega^2)$$

$$= \frac{1}{P^2 |\Omega|^2} \left[(\rho_{11}^2 + \omega^2) D_{PP} + 2\rho_{11}\rho_{21} D_{NP} \right.$$

$$\left. + \rho_{21}^2 D_{NN} \right] \qquad (22)$$

where $\Omega = \omega_R^2 - \omega^2 + j\omega\rho$ is the determinant of the matrix in (21) and $\rho = \rho_{11} + \rho_{22}$ is the damping factor. Usually, one can define the modulation transfer function as $T(\omega) = \omega_R^2/\Omega$, in which $\omega_R^2 = \rho_{12}\rho_{21} + \rho_{11}\rho_{22}$ is the relaxation resonance frequency.

B. Output Relative Intensity Noise

When the quantum features are considered, we should be very vigilant because of the natural quantization properties, such as a photon's particle-like behavior. In this section, we stress that the output photons emitted due to the out-coupling process differ from the intra-cavity photons [13]. The main reason is that each individual photon needs to either be transmitted or reflected when it reaches the laser facet. Although photons with a fixed average rate are reflected back into the laser cavity, this random division finally leads to partition noise with both transmitted and reflected photons [26]. Therefore, it is possible to reuse the Langevin method to describe the outcome of the laser facet partition noise by regarding output photons as another photon reservoir having its own Langevin noise force. In [13] and [15], one can consider them as vacuum fluctuations, which destructively interferes with photons fluctuations. Adapting (21), the output power fluctuations can be expressed with the relation to the intra-cavity photons' RIN:

$$\delta P_{out}(t) = \lambda \delta P(t) + F_{out}(t) \qquad (23)$$

$\lambda = \eta_0 \hbar \omega_0 / \tau_p$ is the fundamental conversion factor between output photons and output optical power. And η_0 is the quantum efficiency of the ICL and $\hbar \omega_0$ the photon energy.
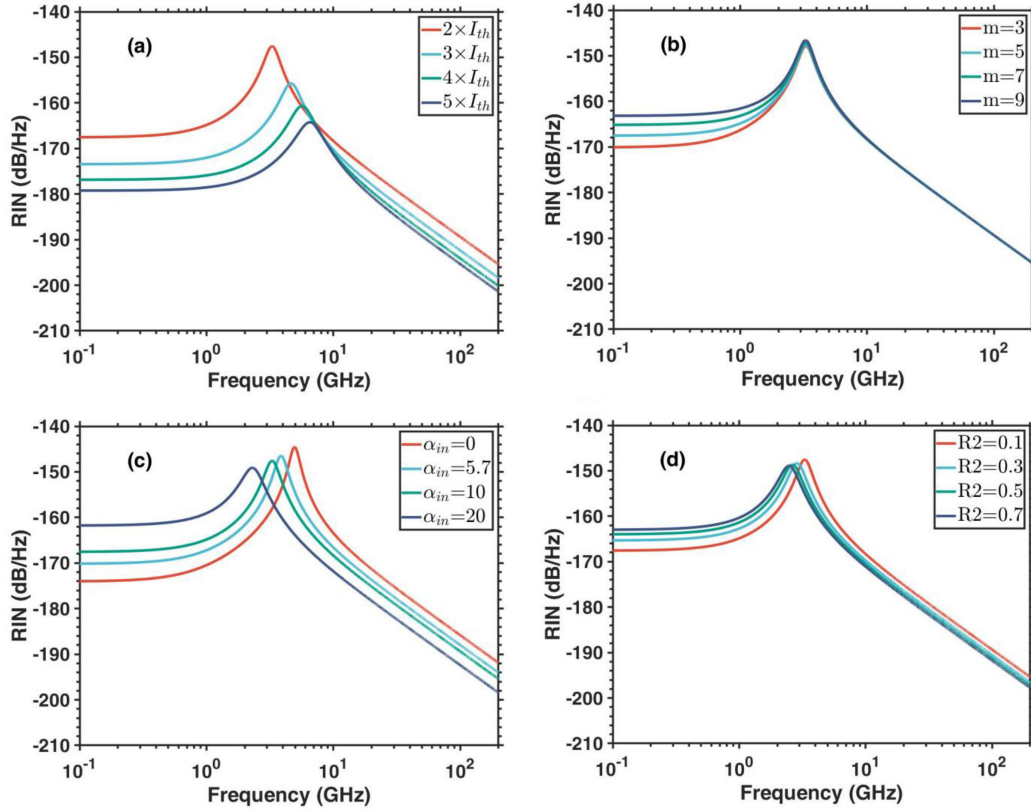
Fig. 3. Intra-cavity RIN spectra (a) for different pump currents while the stage number is fixed at m = 5; (b) for different stage number m while the photon number is fixed at 4.2×10^6; (c) for different internal loss while other parameters stay unchanged; (d) for the laser power reflectivity taking $R_1 = 1$ and R_2 from 0.1 to 0.7.

By utilizing the same method than that in the previous subsection, we convert to the frequency domain by Fourier transform:

$$\langle \delta P_{out}(\omega) \delta P_{out}(\omega)^* \rangle = \lambda^2 \langle \delta P \delta P^* \rangle$$
$$+ 2Re\{\lambda \langle \delta P F_{out} \rangle\} + \langle F_{out} F_{out} \rangle \quad (24)$$

where the first term in this equation is what one would naively expect the relationship to be. However, the partition noise at the laser facet creates two additional noise contributions like vacuum noise sources. Similarly, using Carmer's rule, we can easily show:

$$\langle \delta P F_{out} \rangle = \frac{1}{\Omega}[(\rho_{11} + j\omega) \langle F_P F_{out} \rangle + \rho_{21} \langle F_N F_{out} \rangle] \quad (25)$$

where we suppose

$$\langle F_{out} F_{out} \rangle = \hbar \omega_0 P_0$$
$$\langle F_P F_{out} \rangle = -P_0$$
$$\langle F_N F_{out} \rangle = 0$$

with $P_0 = \lambda P$ the output power of ICL. In addition, one has $\langle F_N F_{out} \rangle = 0$ because it is obvious that there is no correlation between the carrier noise and this partition noise.

TABLE I
MATERIAL AND OPTICAL PARAMETERS OF THE ICLs USED IN THE SIMULATION

Symbol	Description	Value
L	Cavity length	2 mm
W	Cavity width	4.4 μm
$R_1=R_2$	Facet reflectivity	0.32
n_r	Refractive index	3.58
Γ_p	Optical confinement factor	0.04
α_{int}	Internal loss	5.7 cm^{-1}
τ_{aug}	Auger lifetime	1.08 ns
τ_{sp}	Spontaneous emission lifetime	15 ns
τ_p	Photon lifetime	10.5 ps
m	Stage number	5
β	Spontaneous emission factor	1×10^{-4}
a_0	Gain coefficient	2.8×10^{-10} cm^2
N_0	Transparent carrier number	6.2×10^7

IV. RESULTS AND DISCUSSION

Using the above theories, we study the RIN characteristics of an ICL in this section. The material and optical parameters of the ICL used in the simulations are all listed in Table I from the experimental data [19]. Equation (22) reveals that the intra-cavity photon fluctuations follow a $(\alpha + \beta\omega^2)|T(\omega)|^2$ spectral dependence, peaking at the relaxation resonance frequency. This ICL's resonance frequency was recently released in the experiments [27]. The relaxation oscillation of the ICL
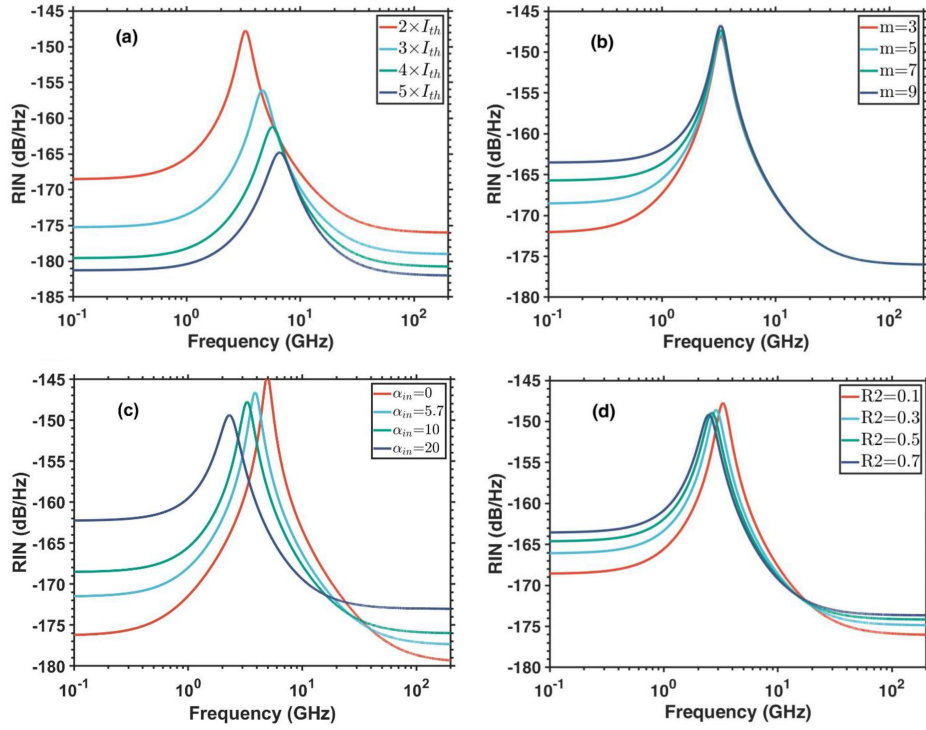
Fig. 4. Output RIN spectra (a) for different pump currents while the stage number is fixed at m = 5; (b) for different stage number m while the photon number is fixed at 4.2×10^6; (c) for different internal loss while other parameters stay unchanged; (d) for the laser power reflectivity taking $R_1 = 1$ and R_2 from 0.1 to 0.7.

is clearly observed in the GHz range, which is large enough to achieve multi-Gbits/s data transmission.

In Fig. 3, the low frequency intra-cavity RIN is found to be steady while above the relaxation resonance, the intra-cavity RIN is reduced even at high frequency. Fig. 3(b) points out that more gain stages slightly improve the intra-cavity RIN due to the uncorrelated photon noise sources in each stage. However, this picture is not enough evidenced for shot-noise limit case. In the following, a new approach is proposed to take into account such effects. Additionally, we also discuss how internal loss and facet reflectivity influence the intra-cavity RIN. In the first place, as seen in Fig. 3(c), more internal loss significantly enhances the intra-cavity RIN, which increases from -174 dB/Hz down to -162 dB/Hz. Furthermore, the low-frequency RIN in Fig. 3(d) declines from -163 dB/Hz for $R_2 = 0.7$ down to -168 dB/Hz for $R_2 = 0.1$. These behaviors can be understood because internal loss and facet reflectivity directly impact the intra-cavity photon lifetime.

If we expand (24) correctly with the Langevin noise correlation strengths and (25), the output RIN has a form of:

$$RIN_{out}(\omega)$$

$$= \frac{\langle \delta P_{out}(\omega) \delta P_{out}(\omega)^* \rangle}{P_0^2} = \frac{\hbar \omega_0}{P_0} \left[\frac{1}{|\Omega|^2} (\alpha' + \beta' \omega^2) + 1 \right]$$

$$= RIN_{in}(\omega) - \frac{2}{|\Omega|^2 P_0} \left[\rho_{11} \omega_R^2 + \rho_{22} \omega^2 \right] + \frac{\hbar \omega_0}{P_0} \quad (26)$$

By comparing $RIN_{in}(\omega)$ and $RIN_{out}(\omega)$, we notice that, in addition to the slightly more complex frequency coefficients, a new "+1" factor appears in $RIN_{out}(\omega)$. This extra factor ensures that the output RIN never drops below the minimum value of $\hbar \omega_0 / P_0$ for all frequencies. This quantum noise floor is often referred to as the standard quantum limit, or the shot-noise floor. The anti-correlation, expressed by the negative sign in the second term of (26), imparts that if a photon is coupled out, the number of intra-cavity photon decreases and the probability of coupling out other photons would also decrease, which reveals the anti-bunching mechanism of the output photons.

Fig. 4 illustrates the characteristics of the output RIN for the ICL under study. As can be seen, the excess noise dominates at low frequency and is remarkably enhanced near the relaxation resonance frequency like the behaviors we observe at intra-cavity RIN. However, ICLs generally quiet down to the standard quantum limit above the resonance at high frequency.

Fig. 4(a) demonstrates that increasing the pump current effectively reduces the output RIN in the whole frequency range including the shot-noise floor. As shown in Fig. 4(b), simulations show that the cascading stage number does not impact the standard quantum limit of ICLs. However, with respect to the internal loss in Fig. 4(c), less internal loss remarkably diminishes the output RIN. It is can also be noted that the effect of the power facet reflectivity stays consistent with the aforementioned results. Therefore, the simulation confirm that these two parameters have a great influence on the shot-noise limit. For example, larger internal loss and more important facet reflectivity increase the shot-noise limit from -180 dB/Hz to -172
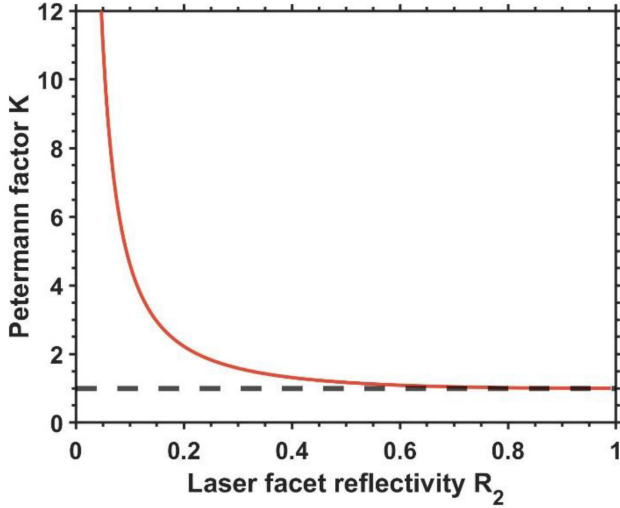
Fig. 5.   Petermann excess noise K factor varies in function of one facet reflectivity R_2 while R_1 is fixed at 1. The black dashed line indicates the K value limit at 1 and is a guide to the eye.
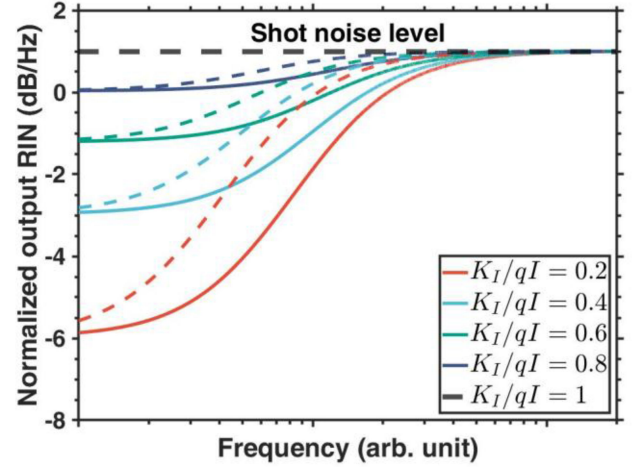

Fig. 6.   Normalized output RIN varies in function of pump current noise. Low frequency noise can be reduced below the standard quantum limit (black dashed line) if the pump current source is "quiet". The colored dashed lines indicate the relatively higher internal loss case ($\alpha_{\text{int}} = 10$) while the solid lines represent $\alpha_{\text{int}} = 5.7$ at the same pumping condition. The pump current is fixed at $2 \times I_{th}$.

dB/Hz. More importantly, the Petermann excess noise K factor can be calculated through (18). Fig. 5 presents the K factor of an asymmetrical Fabry-Perot ICLs, in the case where one of the laser facets is anti-reflective ($R_1 = 1$) meanwhile the other R_2 changes from 0.1 to 1. For high values of R_2, the K factor can be approximated to unity but it becomes very significant for low values of R_2. In a recent study [30], one shows that a minor nonorthogonality of the laser cavity eigenmodes might be an explanation for the bottleneck of the observed squeezing, which means that the intensity noise can hardly be reduced below the standard quantum limit above a critical value of K. This result stresses that ICLs cavity design is of paramount importance for making ultra-low noise light sources.

In the following, we discuss how noise-suppressed pump influences the squeezing performance of the ICLs. In (26), the noise contribution of the current source should appear in α' term in (26). This term can be strongly minimized by using a "quiet" current source [13]. In (26), $\beta'\omega^2|T(\omega)|^2$ is responsible for the RIN peak at ω_R and $\hbar\omega_0/P_0$ dominates the RIN spectrum beyond the peak at high frequency. Consequently, $\alpha'|T(\omega)|^2$ is the only factor that significantly affects the low frequency away from the RIN peak.

Let us now concentrate on the low frequency and suppose that the laser has a perfect quantum efficiency (e.g., $\eta_0 = 1$). Thus at $\omega << \omega_R$, one can set $(\omega_R^2 - \omega^2)^2 \approx \omega_R^4$ without introducing significant error during the calculation. Additionally, we combine the α' term with the factor "+1" within the brackets of (26). With these modifications, the expression of output RIN reduces to:

$$RIN_{out}(\omega) = \frac{\hbar\omega_0}{P_0}\left[\frac{\alpha' + \omega^2\tau_{out}^2}{1 + \omega^2\tau_{out}^2}\right] + \frac{\hbar\omega_0}{P_0}\frac{1}{|\Omega|^2}\beta'\omega^2 \quad (27)$$

where $\tau_{out} = \rho/\omega_R^2$. The first term provides the RIN noise floor, while the second one provides the RIN peak.

The injected current contribution to the output RIN noise spectra can be reduced if a current source with sub-shot-noise characteristics is applied. Yamamoto has already demonstrated that it is not extremely difficult to eliminate the pump-amplitude fluctuation by high-impedance suppression for electron-injection pumping in a semiconductor laser [7]. To accommodate such cases, we can generalize the first term α' in the (26) by K_I/qI and can neglect the second term $\beta'\omega^2|T(\omega)|^2$ because we focus on the low frequency region, where K_I is the spectral density of the injection current. Therefore, it is easy to understand that for a perfectly noise-suppressed or "quiet" current source, $K_I \rightarrow 0$. For a shot-noise limited current source, $K_I = qI$. Fig. 6 demonstrates the amplitude-squeezing effect mentioned above. For a shot-noise limited current source (e.g., $K_I/qI = 1$), the output RIN would stay constant at the standard quantum limit. However, if a nearly noiseless pumping source is applied (e.g., $K_I/qI = 0.2$), the output RIN can be significantly reduced. Therefore, amplitude squeezed states can qualitatively be predicted with compression factors depending on the pump noise conditions.

We can also investigate the role of internal loss in intensity squeezing. Comparing the dashed lines and solid lines in Fig. 6, one may find that more important internal loss value degrades the amplitude-squeezing performance, especially under low pump noise condition. The limited squeezing factor can be explained by the fact that the quantum-mechanical correlation between the laser's internal fluctuation and the reflected vacuum fluctuation becomes imperfect as a result of non-negligible internal loss.

V. CONCLUSION

In conclusion, this work theoretically demonstrates the possibility of producing amplitude-squeezing light from mid-infrared ICLs. A semi-classical rate equation approach is proposed to describe this effect, which is derived from the Green's function method. By considering an additional noise term in the output

power, the relative intensity noise spectra are complemented with the standard quantum limit. In addition, the output relative intensity noise can be reduced at low frequency by utilizing the noise-suppressed pump current source. Although the model remains semi-classical, it allows a qualitative description of the amplitude-squeezing light in semiconductor lasers. According to the simulation results, considerable compression factors of amplitude-squeezing below the standard quantum limit is achievable depending on the pump noise conditions. These theoretical results show a promising way to create sub-shot-noise-limit light in the mid-infrared range that is recently applied in highly precise oscillators, chip-scale gyroscope and laser interferometer gravitational-wave observatory (LIGO) detectors [28]. Future work will involve squeezing experiments and stochastic simulations to analyze the sub-Poissonian output photon number distribution and the corresponding RIN spectra.

REFERENCES

[1] D. F. Walls, "Squeezed states of light," *Nature*, vol. 306, no. 5939, pp. 141–146, 1983.

[2] G. Breitenbach, S. Schiller, and J. Mlynek, "Measurement of the quantum states of squeezed light," *Nature*, vol. 387, no. 6632, pp. 471–475, 1997.

[3] V. Dodonov, "'Nonclassical' states in quantum optics: A 'squeezed' review of the first 75 years," *J. Opt. B: Quantum Semiclassical Opt.*, vol. 4, no. 1, 2002, Art. no. R1.

[4] H. Yuen and J. Shapiro, "Optical communication with two-photon coherent states—Part I: Quantum-state propagation and quantum-noise," *IEEE Trans. Inf. Theory*, vol. 24, no. 6, pp. 657–668, Jun. 1978.

[5] E. Oelker *et al.*, "Ultra-low phase noise squeezed vacuum source for gravitational wave detectors," *Optica*, vol. 3, no. 7, pp. 682–685, 2016.

[6] S. Pirandola, B. R. Bardhan, T. Gehring, C. Weedbrook, and S. Lloyd, "Advances in photonic quantum sensing," *Nature Photon.*, vol. 12, no. 12, pp. 724–733, 2018.

[7] S. Machida, Y. Yamamoto, and Y. Itaya, "Observation of amplitude squeezing in a constant-current–driven semiconductor laser," *Phys. Rev. Lett.*, vol. 58, no. 10, 1987, Art. no. 1000.

[8] J. Mork and K. Yvind, "Squeezing of intensity noise in nanolasers and nanoleds with extreme dielectric confinement," *Optica*, vol. 7, no. 11, pp. 1641–1644, 2020.

[9] R. Q. Yang, "Infrared laser based on intersubband transitions in quantum wells," *Superlattices Microstructures*, vol. 17, no. 1, pp. 77–83, 1995.

[10] L. Dong, C. Li, N. P. Sanchez, A. K. Gluszek, R. J. Griffin, and F. K. Tittel, "Compact CH_4 sensor system based on a continuous-wave, low power consumption, room temperature interband cascade laser," *Appl. Phys. Lett.*, vol. 108, no. 1, 2016, Art. no. 011106.

[11] Y. Deng *et al.*, "Mid-infrared hyperchaos of interband cascade lasers," *Light: Sci. Appl.*, vol. 11, no. 1, pp. 1–10, 2022.

[12] A. Spott *et al.*, "Interband cascade laser on silicon," *Optica*, vol. 5, no. 8, pp. 996–1005, 2018.

[13] Y. Yamamoto, S. Machida, and O. Nilsson, "Amplitude squeezing in a pump-noise-suppressed laser oscillator," *Phys. Rev. A*, vol. 34, no. 5, 1986, Art. no. 4025.

[14] B. Tromborg, H. E. Lassen, and H. Olesen, "Traveling wave analysis of semiconductor lasers: Modulation responses, mode stability and quantum mechanical treatment of noise spectra," *IEEE J. Quantum Electron.*, vol. 30, no. 4, pp. 939–956, Apr. 1994.

[15] J.-L. Vey and P. Gallion, "Semiclassical model of semiconductor laser noise and amplitude noise squeezing. I. description and application to Fabry-Perot laser," *IEEE J. Quantum Electron.*, vol. 33, no. 11, pp. 2097–2104, Nov. 1997.

[16] D. D. Marcenac and J. E. Carroll, "Modeling of intensity noise including squeezing in DFB and Fabry-Perot semiconductor laser diodes," *IEEE J. Quantum Electron.*, vol. 30, no. 9, pp. 2064–2072, Sep. 1994.

[17] J. Arnaud, "Classical theory of laser noise," *Opt. Quantum Electron.*, vol. 27, no. 2, pp. 63–89, 1995.

[18] S. Borri, M. Siciliani de Cumis, S. Viciani, F. D'Amato, and P. De Natale, "Unveiling quantum-limited operation of interband cascade lasers," *APL Photon.*, vol. 5, no. 3, 2020, Art. no. 036101.

[19] Y. Deng and C. Wang, "Rate equation modeling of interband cascade lasers on modulation and noise dynamics," *IEEE J. Quantum Electron.*, vol. 56, no. 2, pp. 1–9, Feb. 2020.

[20] C. Henry, "Theory of spontaneous emission noise in open resonators and its application to lasers and optical amplifiers," *J. Lightw. Technol.*, vol. 4, no. 3, pp. 288–297, 1986.

[21] G.-H. Duan, P. Gallion, and G. Debarge, "Analysis of the phase-amplitude coupling factor and spectral linewidth of distributed feedback and composite-cavity semiconductor lasers," *IEEE J. Quantum Electron.*, vol. 26, no. 1, pp. 32–44, Jan. 1990.

[22] F. Grillot, B. Thedrez, and G.-H. Duan, "Feedback sensitivity and coherence collapse threshold of semiconductor debasers with complex structures," *IEEE J. Quantum Electron.*, vol. 40, no. 3, pp. 231–240, Mar. 2004.

[23] P. M. Morse and H. Feshbach, "Methods of theoretical physics," *Amer. J. Phys.*, vol. 22, no. 6, pp. 410–413, 1954.

[24] B. Tromborg, H. Olesen, and X. Pan, "Theory of linewidth for multi-electrode laser diodes with spatially distributed noise sources," *IEEE J. Quantum Electron.*, vol. 27, no. 2, pp. 178–192, Feb. 1991.

[25] W. Bewley *et al.*, "Lifetimes and auger coefficients in type-II W interband cascade lasers," *Appl. Phys. Lett.*, vol. 93, no. 4, 2008, Art. no. 041118.

[26] L. A. Coldren, S. W. Corzine, and M. L. Mashanovitch, *Diode Lasers and Photonic Integrated Circuits*. Hoboken, NJ, USA: Wiley, 2012.

[27] P. Didier *et al.*, "Relative intensity noise and intrinsic properties of RF mounted interband cascade laser," *Appl. Phys. Lett.*, vol. 119, no. 17, 2021, Art. no. 171107.

[28] G.L. Mansell *et al.*, "Observation of squeezed light in the 2 μm region," *Phys. Rev. Lett.*, vol. 120, no. 20, 2018, Art. no. 203603.

[29] K. Petermann, "Calculated spontaneous emission factor for double-heterostructure injection lasers with gain-induced waveguiding," *IEEE J. Quantum Electron.*, vol. 15, no. 7, pp. 566–570, Jul. 1979.

[30] A. M. Van der Lee, N. J. Van Druten, M. P. Van Exter, and J. P. Woerdman, J.-Ph. Poizat, and P. Grangier, "Critical petermann K factor for intensity noise squeezing," *Phys. Rev. Lett.*, vol. 85, no. 22, pp. 4711–4714, 2000.